

Local approach to fracture based prediction of the ΔT_{56J} and $\Delta T_{K_{Ic,100}}$ shifts due to irradiation for an A508 pressure vessel steel[†].

B. Tanguy^{1,*}, C. Bouchet¹, S. Bugat² and J. Besson¹

¹ *Ecole des Mines de Paris, Centre des Matériaux, UMR CNRS 7633
BP 87, 91003 Evry Cedex, France*

² *EdF les Renardières, Route de Sens - Ecuelles, Moret-sur-Loing 77250, France*

* *Corresponding author. Phone (33) 1.60.76.30.61. Fax: (33) 1.60.76.31.50.*

E-mail address: Benoit.Tanguy@ensmp.fr

[†] *This paper is based on a presentation made at the 15th European Conference of Fracture "Advanced Fracture Mechanics for Life and Safety Assessments" held in Stockholm, Sweden, on August 11-13, 2004*

Abstract

Nuclear pressure vessel steels are subjected to irradiation embrittlement which is monitored using Charpy tests. Reference index temperatures, such as the temperature for which the mean Charpy rupture energy is equal to 56 J (T_{56J}), are used as embrittlement indicators. The safety integrity evaluation is performed assuming that the shift of the nil-ductility reference temperature RT_{NDT} due to irradiation is equal to the shift of T_{56J} . A material model integrating a description of viscoplasticity, ductile damage and cleavage brittle fracture is used to simulate both the Charpy test and the fracture toughness test (CT geometry). The model is calibrated on the Charpy data obtained on an unirradiated A508 Cl.3 steel. It is then applied to irradiated materials assuming that irradiation affects solely hardening. Comparison with Charpy energy data for different amounts of irradiation shows that irradiation possibly also affects brittle fracture. The model is then applied to predict the fracture toughness shifts ($\Delta T_{K_{Ic,100}}$) for different levels of irradiation.

Key words: Irradiation embrittlement; Ductile to brittle transition; Charpy test; Fracture toughness.

1 Introduction

Reactor pressure vessels (RPV) of commercial nuclear power plants are subjected to embrittlement due to the exposure to high energy neutrons from the core. The current way to determine the effects of the degradation by radiation on the

mechanical behavior of the RPV steels is the use of tensile and impact Charpy tests, from which reference index temperatures, such as the ductile to brittle transition (DBT) temperature, can be calculated. More conventionally in the French nuclear surveillance program, T_{56J} , the temperature for which the mean Charpy energy is equal to 56J and its increase due to neutron irradiation are determined. The safety integrity evaluation based on a fracture toughness lower bound curve $K_{Ic}(T - RT_{NDT})$ [1] is then performed assuming that the shift of the nil-ductility reference temperature, RT_{NDT} , is equal to the shift of the embrittlement indicators, e.g. $\Delta RT_{NDT} = \Delta T_{56J}$ for a given fluence. This equivalence is of fundamental importance to structural integrity assessments of RPVs since such assessments are based on fracture toughness properties which are not generally measured directly. However some studies have shown large scatter in the relation between $\Delta T_{K_{Ic}}$ and Charpy index temperature shifts [2, 3]. As the correlation between ΔT_{56J} and $\Delta T_{K_{Ic}}$ is purely empirical, a better understanding is needed. As the same physical mechanisms control the fracture in both Impact V-notch and quasi-static precracked fracture toughness tests, the investigation of this relation using micro-mechanical models of fracture appears to be a very promising way.

The prediction of the Charpy V-notch energies, CVN, and K_{Ic} values vs temperature curves by means of the *Local Approach to Fracture* has led to several studies during the last decade devoted mainly to non-irradiated materials (see among others [4–9]). Within this framework, a micro-mechanical analysis of the Charpy test in order to model the DBT curve was proposed, among others [10], by some of the authors [11, 12].

Assuming that the combined effects of large plastic strain and temperature on the cleavage mechanism lead to a temperature dependence of the average cleavage stress, it is then possible to predict accurately the whole Charpy energy transition curves [12], including the large scatter observed in the DBT range. This strategy allows to transfer the results of the Charpy tests to larger structures and further to study the effect of different damage mechanisms as irradiation or ageing on the DBT temperature. For example in the case of unirradiated materials, the evolution of the elastoplastic fracture toughness can be predicted based on Charpy impact data [9, 13]. The aim of this study is to predict and to compare the irradiation involved shifts of index temperatures obtained from Charpy and fracture toughness tests using a micro-mechanical description of the involved damage processes. The effect of neutron irradiation on hardening properties and embrittlement of reactor pressure vessel steels is analyzed in section 2. The modeling of the ductile to brittle transition is then detailed in section 3 and the hypotheses considered to model the DBT temperature for irradiated materials are presented in section 4. This strategy is then applied to simulate the irradiation-induced shifts of the Charpy DBT curve (section 5) which are then compared to those of the quasi-static fracture toughness (section 6).

2 Effect of neutron irradiation on the Charpy transition curves and hardening properties

For a given fluence (Φ (n.cm⁻²)) of neutrons ($E > 1$ MeV) and irradiation temperature, irradiation induced embrittlement is strongly dependent of the material chemical composition, and specially on Cu, Ni, P contents [14]. The volume fraction of copper is an important factor in the hardening-induced embrittlement due to the irradiation induced defects. This has led to consider these chemical elements in the empirical embrittlement correlation models for the prediction of the shift of the reference index temperatures [15, 16]. On the physical point of view, irradiation produces fine scale microstructures [17]. Their effects on the macroscopic behavior can be separated into two groups [17, 18]: (i) change of the plastic hardening, (ii) embrittlement, one of the most well-known and well-described being phosphorous segregation at grain boundaries [17]. Hardening mechanisms include matrix and age hardening. Matrix hardening is due to radiation-produced point defect clusters and dislocation loops, referred to as the matrix damage contribution [18]. Age hardening is an irradiation-enhanced formation of copper-rich precipitates. These two hardening mechanisms cause an increase of the yield strength whereas phosphorous segregation causes grain boundaries embrittlement without any increase of hardness and may be responsible for intergranular fracture [19]. It should be underlined that the micromechanical models developed in this study do not consider the embrittlement of the grain boundaries due to phosphorous segregation. Intragranular cleavage is assumed to be the prevailing mechanism controlling brittle fracture.

Two principal types of irradiation-induced hardening were found in the literature and are schematically represented on fig. 1a. In the first case (dashed curve

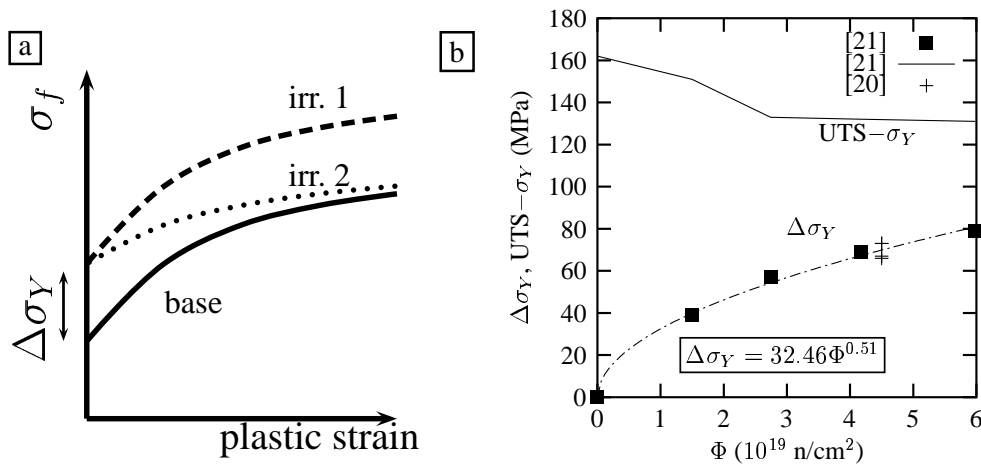


Fig. 1. a) Two principal hypotheses concerning the evolution of the flow stress after neutron irradiation. b) Evolution of $\Delta\sigma_Y$ and $UTS - \sigma_Y$ as a function of the irradiation flux for an A508 Cl.3 steel (base metal) ($T_{test} = 300^\circ\text{C}$) [21].

labeled irr. 1) the whole stress-strain curve of the unirradiated material is shifted to higher stress values by $\Delta\sigma_Y$, i.e. the strain hardening rate remains unchanged whereas the yield stress is increased [22, 23]. This case was also experimentally observed on ferritic alloys irradiated at 288°C by electron irradiation [24]. In the second case the yield stress is increased by $\Delta\sigma_Y$ whereas the ultimate tensile stress (UTS) remains almost unaffected by irradiation (dotted curve labeled irr. 2), i.e. that the hardening rate is substantially lower than in the unirradiated conditions. This case is reported for steels (ferritic, martensitic) subjected to neutron irradiation at low temperatures ($\leq 200^\circ\text{C}$) [25] and its importance increases with decreasing irradiation temperature [26]. At high irradiation doses, it is also suggested that neutron irradiation has a similar effect as a plastic prestrain on strain hardening [27].

The choice of the appropriate case is undoubtedly strongly dependent on the considered material: in pioneer studies on the interpretation of irradiation effects on low temperature fracture toughness, the second case was considered for an A533B steel [28] whereas it was the first case for an A508 Cl.3 steel in [23]. The variation of the yield stress and the difference between the ultimate stress and the yield stress for an A508 Cl.3 steel from the French surveillance program [20, 21] with a chemical composition very close to the unirradiated A508 Cl.3 material considered in this study [29] and their evolutions with irradiation fluence are reported on fig. 1b. The variation of the yield stress with fluence up to a maximum value of $6.0 \cdot 10^{19}\text{n/cm}^2$ is well represented by a power-law expression, $\Delta\sigma_Y = h\Phi^n$. A value of 0.51 is obtained for n which is representative of the low doses regime where the work hardening behavior is not altered by irradiation [25, 30]. Data plotted on fig. 1b show that for fluence up to 6.10^{19}n/cm^2 (i.e. $\Delta\sigma_Y \sim 80\text{ MPa}$) the behavior of the investigated steel is closer to case irr-1 which however slightly overestimates the actual UTS¹. Therefore the hypothesis of unaltered work hardening behavior will be the only one considered in the present study. This will lead to higher computed stresses.

Considering both the impact and fracture toughness properties, it is well known that irradiation embrittlement induces an increase of the DBT temperature and therefore of the index T_{56J} [2, 17, 19, 23, 28, 31]. As far as the upper shelf energy (USE) is concerned, most of the studies report a decrease with increasing irradiation level. This decrease being strongly dependent of the material considered for a given level of irradiation. Based on experimental evidences, linear correlations between the yield stress increase and the DBT temperature shift on the Charpy energy curves, $\Delta T_X = \alpha_X \Delta\sigma_Y$, have been proposed in the literature. In the French surveillance program, the shift of the index $T_{56J}(\Phi)$ is considered [19] whereas $T_{41J}(\Phi)$ is used in the American regulations. Based on the experimental values given in [14, 19, 21, 32] where only A533B and A508 Cl.3 structural steels are considered linear correlations between ΔT_{56J} , ΔT_{41J} and $\Delta\sigma_Y$ for various RPV base metals were established: $\Delta T_{56J} = 0.60\Delta\sigma_Y$ and $\Delta T_{41J} = 0.53\Delta\sigma_Y$ (see

¹ Rigorously, the variation of the ultimate stress is given by $\Delta UTS = 19.3\Phi^{0.51}$ showing that the hardening rate is slightly decrease with increasing level of irradiation.

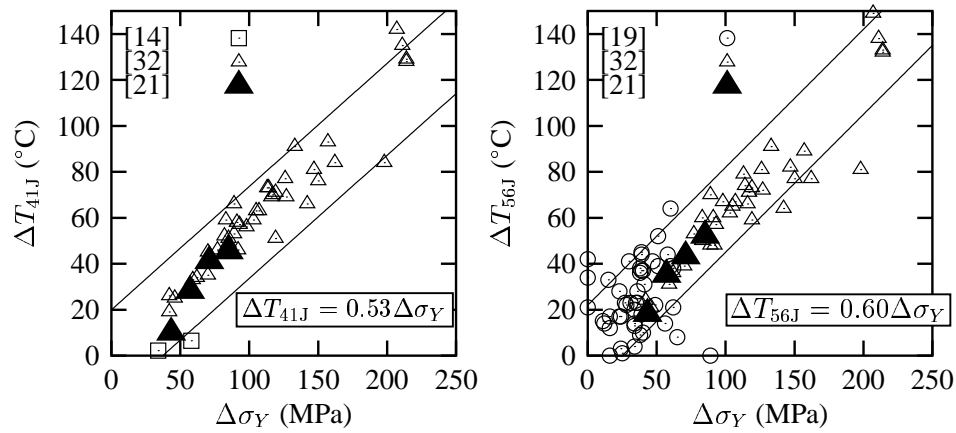


Fig. 2. Evolution of temperature indexes, ΔT_{41J} and ΔT_{56J} as a function of $\Delta\sigma_Y$ for various RPV base metals.

fig. 2).

The established $\Delta T_{56J} = f(\Delta\sigma_Y(\Phi))$ correlation will be considered as the reference experimental database to which the predictions developed in this study for Charpy tests will be compared. For fracture toughness tests, the level of $100 \text{ MPa}\sqrt{\text{m}}$, which is also considered in the Master curve approach [33, 34] to define the reference temperature, T_0 , will be used. The finite element (FE) simulations of fracture toughness tests for different levels of irradiation will be then used to determine the shift of the index $\Delta T_{K_{Ic},100}$. These predicted shifts will be then compared to the shift of impact toughness ΔT_{56J} .

3 Modeling of the ductile to brittle transition

The behavior of the reference unirradiated A508 Cl.3 steel of this study is presented in the following. More details can be found in [12, 29, 35]. The material model consists of three parts: (i) a temperature and strain rate dependent viscoplastic model describing the behavior of the undamaged material, (ii) a model for ductile tearing, (iii) a model for transgranular cleavage fracture.

3.1 Viscoplastic behavior and ductile failure

A modified Rousselier model [36] which is able to handle strain rate and temperature dependence of the material behavior is used to represent ductile failure. In this model, as in the well-known GTN model [37], a single damage parameter which represents the void volume fraction, f , is used to model ductile fracture.

The model is based on the implicit definition of an effective stress (σ_*) which is a function of both the macroscopic Cauchy stress ($\underline{\sigma}$) and of the porosity:

$$\frac{\sigma_{\text{eq}}}{(1-f)\sigma_*} + \frac{2}{3}fD_R \exp\left(\frac{q_R}{2} \frac{\sigma_{\text{kk}}}{(1-f)\sigma_*}\right) - 1 \stackrel{\text{def. } \sigma_*}{=} 0 \quad (1)$$

where σ_{eq} is the von Mises equivalent stress and σ_{kk} the trace of the stress tensor, while q_R and D_R are material parameters which need to be adjusted.

The viscoplastic yield function is written as:

$$\phi = \sigma_* - R(p). \quad (2)$$

where the flow stress R as a function of the effective plastic strain, p is given by:

$$R(p, T) = \sigma_Y(T) + Q_1(T)(1 - \exp(-b_1(T) \times p)) + Q_2(1 - \exp(-b_2 \times p)) \quad (3)$$

where the yield stress $\sigma_Y(T)$, $Q_1(T)$ and $b_1(T)$ are temperature dependent. The values of the parameters of eq. 3 can be found in [12]. Viscoplastic flow occurs when $\phi \geq 0$. The equivalent plastic strain rate \dot{p} is given by the viscoplastic flow function $\dot{p} = \mathbf{F}(\sigma - R)$ which is expressed as:

$$\frac{1}{\dot{p}} = \frac{1}{\mathbf{F}} = \frac{1}{\dot{\varepsilon}_1} + \frac{1}{\dot{\varepsilon}_2} \quad \text{with} \quad \dot{\varepsilon}_i = \left\langle \frac{\sigma_* - R}{K_i} \right\rangle^{n_i} \quad i = 1, 2 \quad (4)$$

The strain rates $\dot{\varepsilon}_1$ and $\dot{\varepsilon}_2$ are each representative of a deformation mechanism: (1) Peierls friction, (2) phonon drag. Deformation is controlled by the slowest mechanism. Here it is important to underline that the viscoplastic model is identified in the whole range of strain rates (10^{-4} up to 4000 s^{-1}), temperatures (-196 up to 300°C) and plastic strains (up to 1.0 using the Bridgman analysis) encountered during the Charpy test and the quasi-static fracture toughness test in the whole DBT range including fully ductile behavior.

The plastic strain rate tensor is given by the normality rule as:

$$\dot{\underline{\varepsilon}}_p = (1-f)\dot{p} \frac{\partial \phi}{\partial \underline{\sigma}} = (1-f)\dot{p} \frac{\partial \sigma_*}{\partial \underline{\sigma}}. \quad (5)$$

The evolution of the damage variable is governed by mass conservation modified to account for nucleation of new voids [37, 38]:

$$\dot{f} = (1-f)\text{trace}(\dot{\underline{\varepsilon}}_p) + A_n \dot{p}. \quad (6)$$

In this expression, the first right handside term corresponds to void growth and the second one to strain controlled nucleation. A_n is a material parameter representing the nucleation rate [39]. All model parameters directly related to ductile fracture

(i.e. q_R , D_R and A_n) are assumed to be temperature independent.

Under quasi-static loading, isothermal conditions are assumed. Under rapid loading corresponding to adiabatic conditions, the temperature T increases due to plastic deformation. In the following, the temperature evolution is written as:

$$C_p \dot{T} = \beta \dot{\underline{\epsilon}}_p : \underline{\sigma} = (1 - f) \beta \dot{p} \sigma_* \quad (7)$$

where C_p is the volume heat capacity and β a constant factor. Note that C_p equals $(1 - f)C_p^0$ where C_p^0 is the heat capacity of the undamaged material so that $C_p^0 \dot{T} = \beta \dot{p} \sigma_*$.

The constitutive equations lead to softening up to crack initiation and propagation so that a material scale length is required. In the following, this length, l , is identified to the mesh size which must be adjusted. As the model parameters are numerous, some of them were directly obtained from the metallurgical analysis of the material. In the present case, the initial porosity is set equal to the Manganese sulfide (MnS) inclusions volume fraction (i.e. $f_0 = 1.75 \cdot 10^{-4}$). Cross section examinations of notched bars and Charpy specimen, show that secondary voids are nucleated on cementite particles (Fe_3C) at high levels of plastic strain. Nucleation starts for $p \approx 0.5$ [29]. The carbide volume fraction is obtained from the chemical composition of the material: 2.3%. This sets the maximum value of the nucleated porosity. Nucleation is assumed to end for $p \approx 1.1$ which is the level of plastic deformation in a tensile bar close to the rupture surface. Consequently the nucleation rate parameter A_n (eq. 6) is set to 0.038 for $0.5 \leq p \leq 1.1$ et to 0.0 otherwise. The other parameters were obtained fitting the model on experimental results from notch tensile bars (NT) with different notch radii at room temperature [12]. The following model parameters were used: $q_R = 0.89$, $D_R = 2.2$ and $l = 100 \mu\text{m}$.

3.2 Brittle failure

The description of brittle failure is derived from the Beremin model [40] which assumes the well-accepted assumption that cleavage is controlled by the propagation of the weakest link among a pre-existing population of statistically size-distributed microcracks. The model uses the following definition of a local effective stress for brittle failure σ_{Ip} :

$$\sigma_{Ip} = \begin{cases} \sigma_I \exp(-p/k) & \text{if } \dot{p} > 0, p > p_c \\ 0 & \text{otherwise} \end{cases} \quad (8)$$

where σ_I is the maximum principal stress of $\underline{\sigma}$. The condition $\dot{p} > 0$ expresses the fact than failure can only occur when plastic deformation occurs. The $\exp(-p/k)$ term has been proposed in [40] to phenomenologically account for grain shape changes or crack blunting induced by plastic deformation. p_c is the critical strain

over which cleavage can occur. This brittle failure model can be applied as a post-processor of calculations including ductile tearing. In this case, care must be taken while computing the failure probability as ductile crack advance leads to unloading of the material left behind the crack front. Considering that each material point is subjected to a load history, $\underline{\sigma}(t)$, $p(t)$ ($t = \text{time}$) the probability of survival of each point at time t is determined by the maximum load level in the time interval $[0, t]$. An effective failure stress $\tilde{\sigma}_{Ip}$ is then defined as:

$$\tilde{\sigma}_{Ip}(t) = \max_{t' \in [0, t]} \sigma_{Ip}(t') \quad (9)$$

The failure probability, P_R , is obtained by computing the Weibull stress, σ_w :

$$\sigma_w = \left[\int_V \tilde{\sigma}_{Ip}^m \frac{dV}{V_0} \right]^{1/m} \quad P_R = 1 - \exp \left[- \left(\frac{\sigma_w}{\sigma_u} \right)^m \right] \quad (10)$$

where the volume integral is taken over the whole volume of the specimen. V_0 is a reference volume which can be arbitrarily fixed. m is the Weibull modulus which describes the scatter of the distribution, σ_u is a scaling parameter which can be interpreted as a measure of the mean cleavage strength of a reference volume V_0 . Model parameters (σ_u , m , k , p_c) must be adjusted.

The original model is adapted to account for the temperature dependence of the model parameters [12]. The rupture probability of a volume element is then no longer represented by σ_{Ip} but by $\omega = (\sigma_{Ip}/\sigma_u)^m$ where both σ_u and m may be temperature dependent. The load history integrating stress variations but also temperature changes is represented by:

$$\tilde{\omega}(t) = \max_{t' \in [0, t]} \omega(t') \quad (11)$$

Finally the failure probability is given by:

$$P_R(t) = 1 - \exp(-\Omega(t)) \quad \text{with} \quad \Omega(t) = \int_V \tilde{\omega}(t) \frac{dV}{V_0}. \quad (12)$$

The parameters of the model for brittle fracture have been identified using NT bars tested at low temperature ($T \leq -150^\circ\text{C}$): $m = 17.8$, $k = 4$, $p_c = 0$ and $\sigma_u = 2925 \text{ MPa}$ for $V_0 = 100 \mu\text{m}^3$.

3.3 Ductile to brittle transition

The ductile to brittle transition is modeled by simulating ductile tearing and by post-processing the results in order to obtain the brittle failure probability. There is therefore no specific model for the transition. This methodology has shown

to be able to predict mean values as well as scatter of impact and quasi-static Charpy energies from low temperatures up to -80°C (including the 56 Joules level of impact Charpy energy) using the cleavage model parameters identified at low temperatures ($T \leq -150^{\circ}\text{C}$), i.e. with constant values for these parameters. However it is necessary to introduce a temperature dependent σ_u parameter above a threshold temperature ($\approx -80^{\circ}\text{C}$) to model the sharp upturn of the Charpy transition curve and to describe the upper part of the curve [12] (Fig. 5).

This apparent effect of temperature on the cleavage mechanism which maybe combines the effects of large plastic strain, temperature-induced inhomogeneities of local stress-strain fields [41] and a possible change of the critical defects population is not within the scope of this paper and is under investigation.

4 Simulation of the ductile to brittle transition for irradiated materials

All the simulations presented here are conducted using the implicit finite element code ZeBuLon [42]. The FE meshes used to simulate the Charpy and the Compact tension specimens are shown on fig. 3. Details can be found in [12]. For both

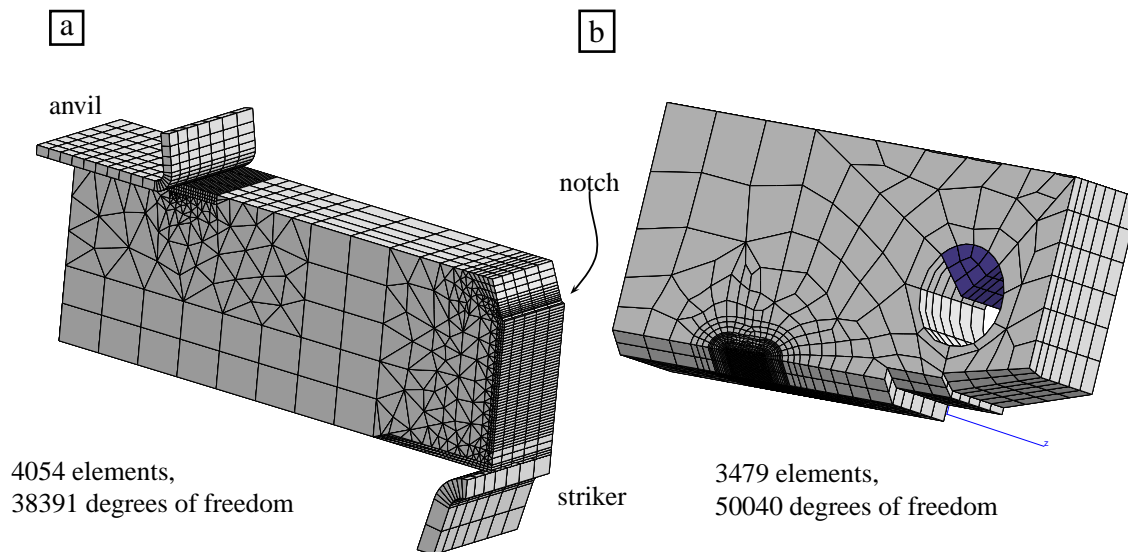


Fig. 3. Finite element meshes used for the analysis. a) Charpy specimen b) CT specimen.

specimens only $\frac{1}{4}$ is meshed due to symmetries. The Charpy specimen, striker and anvil sizes and geometries are those of the AFNOR standard [43]. For the CT specimens an initial crack ratio $a_0/W = 0.55$ has been considered. Full 3D computations have been carried out for both geometries.

Using the previously described models and the hypothesis that the effect of neutron irradiation on DBT temperature shifts can be quantitatively assessed in terms of the effects of irradiation on the flow properties of the material, it becomes

possible to model the effect of irradiation on the ductile to brittle transition and to quantitatively forecast the Charpy energy or fracture toughness versus temperature curves. Obviously the increase of the flow stress has two consequences: (i) stresses in the material increase causing earlier brittle failure, (ii) the macroscopic load on the Charpy specimen increases causing an increase of the dissipated energy in the ductile regime so that the USE also increases. The USE is computed by propagating the ductile crack through the whole Charpy specimen. It is here assumed that the ductile and cleavage micromechanisms are not affected by irradiation. Based on literature results this assumption is discussed in the following sections.

4.1 *Effect of irradiation on ductile damage mechanisms*

Studies of ductile damage mechanisms sensibility to irradiation are seldom in the published literature. The possible effect of irradiation on ductile damage has to be considered through the nucleation, growth and coalescence processes.

Nucleation. At a nano-scale level, numerous experiments on RPV steels, using techniques as small angle neutron scattering (SANS) [44] or atom probe analysis [45], have reported the creation of irradiation induced defects. Considering their mean size (few nm) it is unlikely they can act as potential nuclei for ductile damage. This assumption seems to be confirmed by the micrographs of fracture surfaces of irradiated Charpy specimen tested in the upper-shelf domain [46, 47]. On these micrographs the mean size of the ductile voids appears to be of the order of few microns. Assuming that these voids have nucleated around nanosize precipitates would imply a void growth ratio of about 200 which is unrealistic. On the other hand the observed dimple size is characteristic of voids nucleated around carbides in such steels. Results concerning the irradiation effect on carbides are more ambiguous and seem to be strongly dependent on the chemical composition of the considered steel. In the case of French ferritic pressure vessel steels, it has been shown that no change in composition and size of M_2C or M_3C carbides can be attributed to the irradiation process [48]. The last population of particles to be considered is the MnS inclusions. Previous studies on A503 Cl.3 steels have shown that the void nucleation from such inclusions occurs for a very low deformation ($< 2\%$) [49] so that it can be considered as voids present in the virgin material. Therefore it is unlikely that irradiation will affect the void nucleation process of MnS. Based on these results, it is considered that the nature of defects involved in the nucleation process are unchanged by irradiation. Lacking of studies devoted to the correlation between the carbides void nucleation rate and irradiation has led to keep the void nucleation law established for the unirradiated material unchanged (eq. 6). However it should be kept in mind that an increase of the void nucleation rate may be due to irradiation as it was considered in [50] for vanadium alloyed RPV steels. In this study [50] it was considered that the

segregation of phosphorous on carbide and non-metallic inclusion interfaces reduce the critical void nucleation strain. So that both the nucleation rate and total nucleated volume fraction are increased.

Growth. At a continuum scale changes of hardening properties may have an influence of the growth process of existing cavities issued from large inclusions. Cell computations [51] have shown that when the hardening rate remains unchanged, as it is almost the case for the steel considered in this study, there is little effect on void growth kinetic so that the model parameters are kept constant.

Coalescence. As the hardening rate of the studied material is not strongly affected by irradiation, at a first approximation it was considered that the localization kinetic which controls the coalescence process is not irradiation dependent. Nevertheless it is reminded that in case of high irradiation doses dislocation channel deformation develops and promotes strain localization. Moreover additional irradiation-induced precipitates between large voids issued from inclusions, as sulfides, are likely to change the coalescence process as described in [52].

4.2 *Effect of irradiation on transgranular cleavage mechanisms*

In the case of cleavage fracture, it has been often considered that at low temperatures the critical cleavage stress is not affected by irradiation [23, 28] provided the fundamental mechanism remains identical, i.e. stress propagation-controlled transgranular cleavage. It is often argued in the literature that for ferritic steels the local critical cleavage stress, σ_c , is controlled by the coarse-scale trigger particle microstructure and by the microarrest toughness, k_{ic} , of the ferrite matrix [53] and that fine scale irradiation induced features are not expected to have an influence on σ_c and k_{ic} . Therefore the mean cleavage fracture stress will be first considered as independent on irradiation. Considering the cleavage model presented in section 3.2 it means that all the model parameters are unaffected by irradiation.

4.3 *Effect of irradiation on the temperature dependence of the yield stress*

In order to simulate the whole DBT curve, FE modeling of Charpy-V notch and CT specimens have been carried out in the temperature ranges $[-140^{\circ}\text{C} : +100^{\circ}\text{C}]$ and $[-100^{\circ}\text{C} : +100^{\circ}\text{C}]$, respectively. The increase of yield stress due to irradiation in the whole temperature range investigated is then needed. A first approach is to consider that the hardening observed at one temperature is the same in the whole temperature range [3, 23]. This relies on the fact that the microstructures produced by both matrix- and age-hardening provide only long-range barriers to dislocation motion whereas the temperature dependence of the flow properties is controlled

by the lattice spacing so that the thermal part of the yield stress should be weakly affected by irradiation. However experimental data published in the literature show a slight modification of the yield stress temperature dependence with irradiation especially at low temperatures [21, 54, 55]. Using these experimental data the yield stress can be expressed as a function of the temperature and of the fluence as

$$\sigma_Y(\Phi, T) = \sigma_Y(\Phi = 0, T) + \Delta\sigma_Y(\Phi, T = 300) \times g(T) \quad (13)$$

where $g(T)$ is given by:

$$g(T) = 1 + 0.83 \exp\left(-\alpha_1 \frac{T}{T_0}\right) - 0.616 \exp\left(-\alpha_2 \frac{T}{T_0}\right) \quad (14)$$

with $\alpha_1 = 2.81$, $\alpha_2 = 3.0$ and $T_0 = 273.15^\circ\text{C}$.

5 Simulation of the irradiation-induced shifts of the Charpy DBT curve

In a previous study [56], the Charpy transition curve was simulated for different values of $\Delta\sigma_Y$, i.e. for different levels of irradiation, equal to 45 (low irradiation level), 88 (mean irradiation level) and 150 MPa (high irradiation level). For irradiation levels higher than those reported on fig. 1b and up to $\Delta\sigma_Y = 150$ MPa, it is assumed that the saturation in irradiation hardening is not reached and that the deformation mode remains unchanged [25, 57] (i.e. no dislocation channel deformation). Results for the shifts obtained on the reference temperatures, ΔT_{56J} and ΔT_{41J} are reported on Fig. 4.

As the trends observed for both temperature indexes are similar, comments will focus on the ΔT_{56J} index (Fig. 4a). For the three values of $\Delta\sigma_Y$, it is shown that ΔT_{56J} is always underestimated assuming that the temperature dependent value of $\sigma_u(T)$ is unaffected by irradiation (dotted line in fig. 4a). Assuming that σ_u is a constant equal to the low temperature value for the unirradiated material (2925 MPa) gives a conservative estimation of ΔT_{56J} (dashed line in fig. 4a). Up to a value of about $\Delta\sigma_Y = 88$ MPa, the model gives an estimation which corresponds to the upper band of the experimental data. To obtain the mean temperature shift given in fig. 2b, the parameter σ_u has to be assumed to be also affected by irradiation (full line in fig. 4a). The parameter for the irradiated material is then expressed as: $\sigma_u^{\text{irr}} = \sigma_u(T + \Delta T_\Phi)$.

The shift ΔT_Φ depends on the level of irradiation, it is calculated in order to represent the experimental correlation between ΔT_{56J} and $\Delta\sigma_Y$ (Fig. 2b) and is given in fig. 5 for the three values of $\Delta\sigma_Y$. It is shown in fig. 4b, that the prediction for ΔT_{41J} is in reasonable agreement with experimental bounds up to the maximum $\Delta\sigma_Y$ considered in this study (150 MPa) using the same $\sigma_u(T + \Delta T_\Phi)$ function.

Using the $\sigma_u(T + \Delta T_\Phi)$ variation shown on fig. 5, the predicted Charpy curves

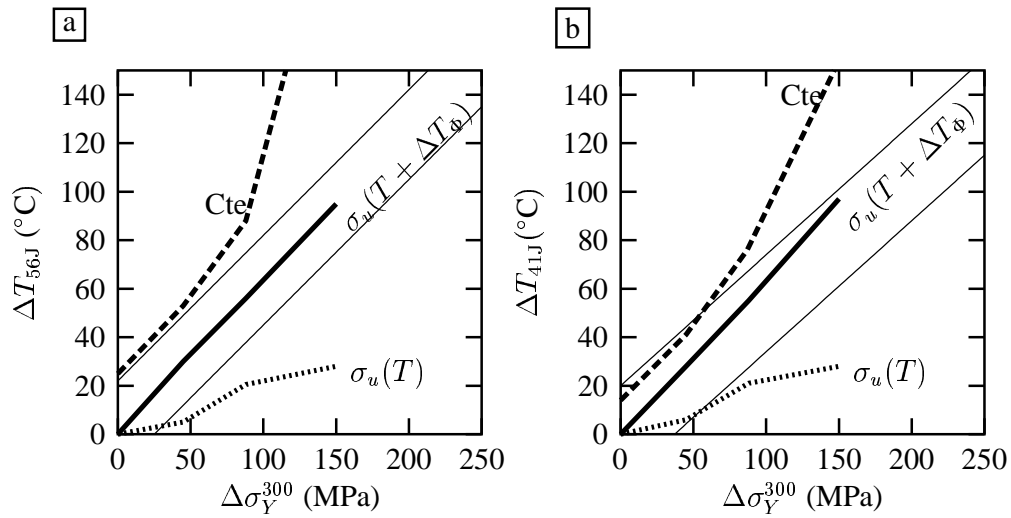


Fig. 4. Prediction of ΔT_{56J} and ΔT_{41J} . Three hypotheses are used for the parameter σ_u : (i) constant value (low temperature value for the unirradiated material), (ii) temperature dependent σ_u (unirradiated material), (iii) temperature and irradiation dependent σ_u (Fig. 5). Thin lines recall the experimental range.

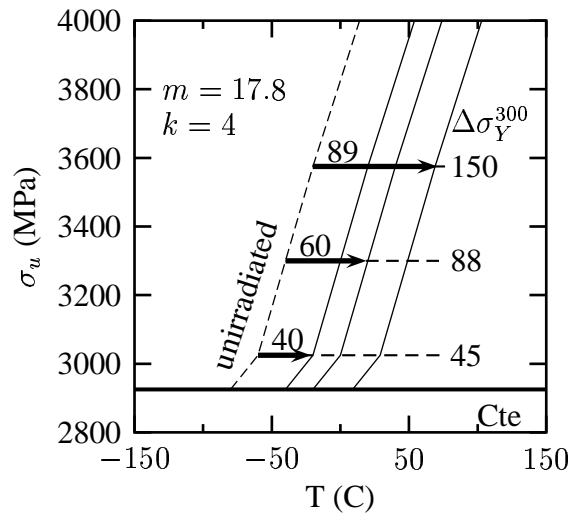


Fig. 5. Variation of σ_u as a function of temperature for the unirradiated material and for irradiation levels corresponding to an increase of the yield stress equal to 45, 88 and 150 MPa. Arrow indicates the temperature shift, ΔT_ϕ , caused by irradiation.

corresponding to a 50% cleavage failure probability for the considered $\Delta\sigma_Y$ values are reported on fig. 6. On this figure the predicted Charpy energies corresponding to a ductile crack propagation of 0.2 and 0.5 mm are also drawn. The simulation results show that the energy level of 56J (drawn with an arrow on each graph) corresponds to a ductile tearing between 0.2 and 0.5 mm. It is therefore necessary

to take into account ductile damage to numerically estimate the shift of the index T_{56J} .

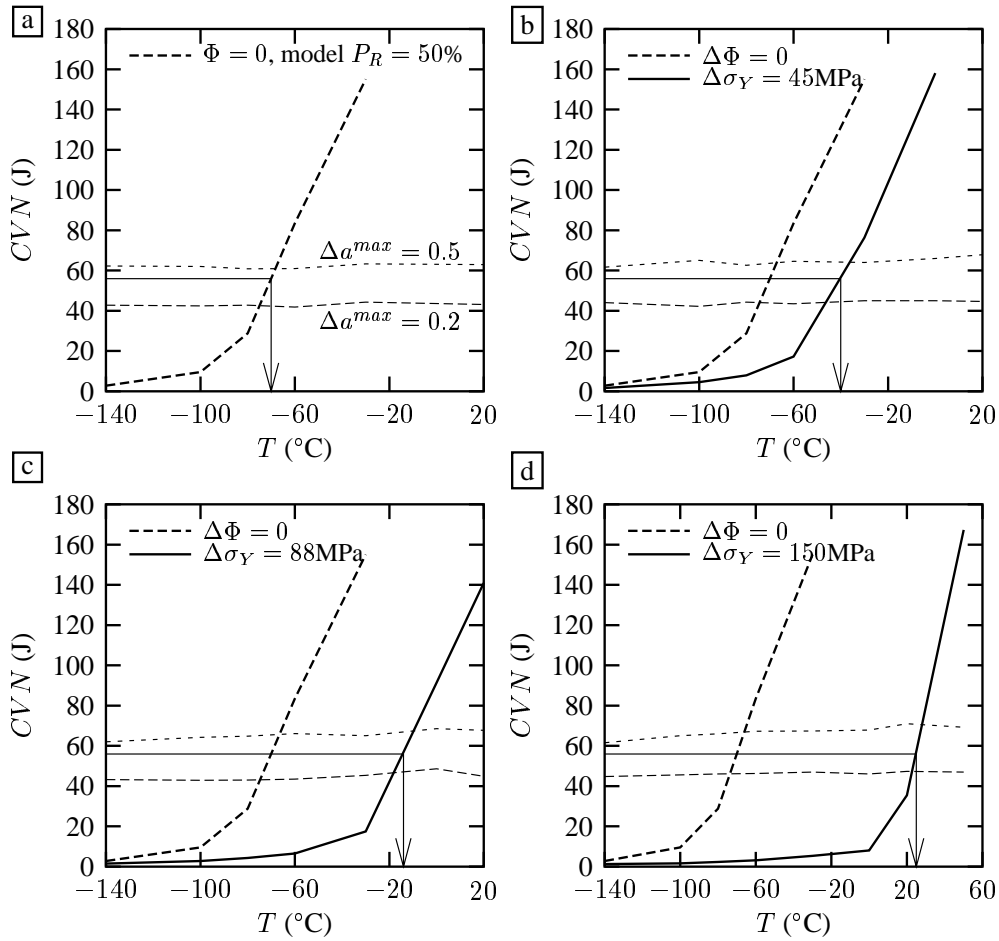


Fig. 6. Comparison of the unirradiated and irradiated predicted Charpy energy curves corresponding to a 50 % cleavage failure probability as a function of temperature for different irradiation-induced increases of the yield stress, $\Delta\sigma_Y$. a) unirradiated material, b) $\Delta\sigma_Y = 45$ MPa, c) $\Delta\sigma_Y = 88$ MPa, d) $\Delta\sigma_Y = 150$ MPa. The calculated temperature corresponding to a 56J level are indicated by an arrow on each graph. CVN energy levels corresponding to a ductile tearing of 0.2 and 0.5 mm are drawn with thin dashed lines on each graph.

6 Simulation of the irradiation-induced shifts of the fracture toughness DBT curve

The same methodology has been applied to simulate the irradiation-induced shifts of the fracture toughness curve: the evolution of σ_u^{irr} determined to fit the $\Delta T_{56J} - \Delta\sigma_Y$ correlation was applied to predict the shift of $T_{K_{Ic,100}}$ as a function of $\Delta\sigma_Y$.

The ability of the model to predict fracture toughness for the unirradiated material using the $\sigma_u(T)$ relation obtained from Charpy data was shown in a previous study [13] and is reported on fig. 7a. As in this study no tests have been performed on irradiated A508 Cl.3 steel, data from literature on similar A508 Cl.3 steels [20, 23] were used for comparison with the model predictions. The effect of irradiation on the shifts of the reference temperature, $T_{K_{Ic},100}$ is reported on fig. 7b, c and d.

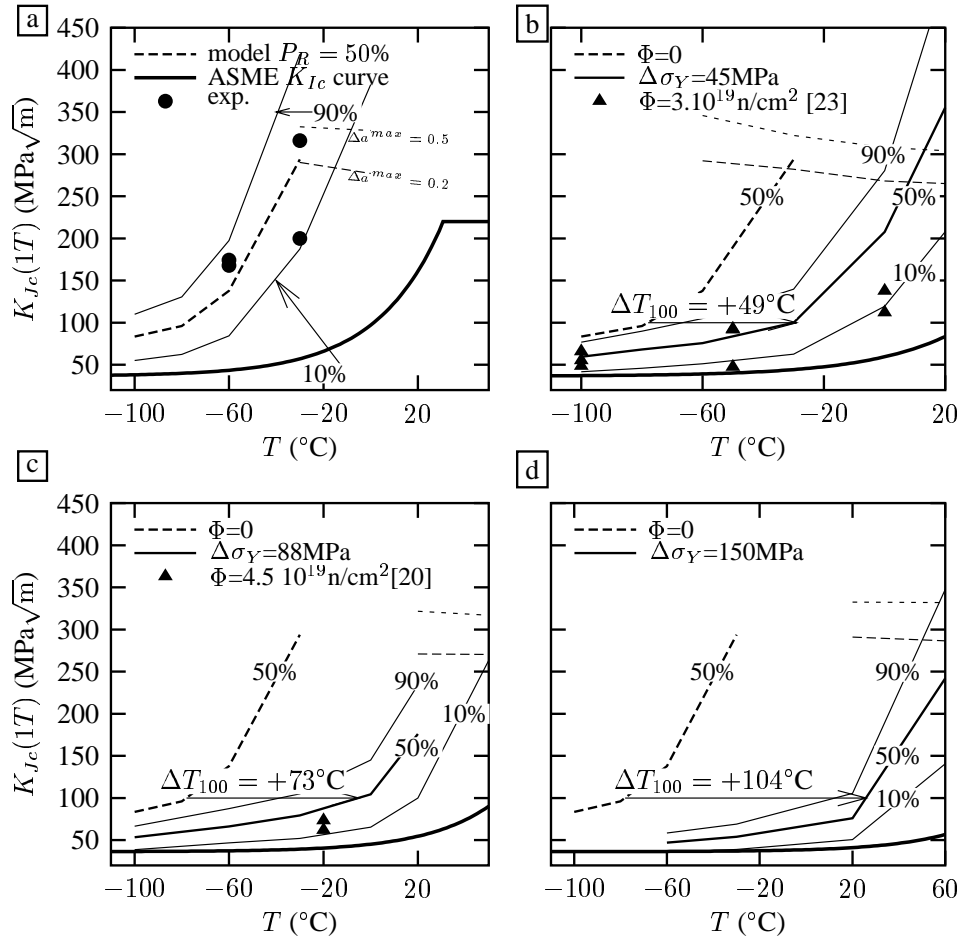


Fig. 7. Comparison of the unirradiated and irradiated predicted fracture toughness curve bounds ($P_r = 10, 50, 95\%$) of as a function of temperature for different irradiation-induced increases of the yield stress, $\Delta\sigma_Y$. a) unirradiated material, b) $\Delta\sigma_Y = 45$ MPa, c) $\Delta\sigma_Y = 88$ MPa, d) $\Delta\sigma_Y = 150$ MPa. The calculated temperature shifts at $100 \text{ MPa}\sqrt{\text{m}}$ referring to the unirradiated state are reported on each graph. The ASME K_{Ic} curves are represented with thick line ($RT_{NDT}^{unirr} = -27^\circ\text{C}$). Fracture toughness levels corresponding to a ductile tearing of 0.2 and 0.5 mm are drawn with thin dashed lines on each graph.

For $\Delta\sigma_Y = 45$ and 88 MPa, a good agreement is obtained between the model predictions and available experimental data (see fig. 7 b and c). The fracture toughness levels corresponding to a ductile tearing of 0.2 and 0.5 mm are also

shown on fig. 7. It appears that for a level of $100 \text{ MPa}\sqrt{\text{m}}$ from which the shift of the toughness curve is obtained, ductile damage has not started to develop, the hypotheses concerning the irradiation effect on ductile damage do not have an influence on the predicted $\Delta T_{K_{Ic},100}$.

The $\Delta T_{K_{Ic},100}$ shift values obtained considering the 50% failure probability prediction are reported on each graph and a comparison with ΔT_{56J} is made in tab. 1. The predicted $\Delta T_{K_{Ic},100}$ values are slightly higher than the shifts ΔT_{56J} , i.e. ΔRT_{NDT} . The difference decreases with increasing $\Delta\sigma_Y$.

Nevertheless as the predicted $\Delta T_{K_{Ic},100}$ shifts are more important than the ΔT_{56J} shifts (ΔRT_{NDT}), the conservatism of the ASME K_{Ic} curve has to be checked for the irradiated material. The ASME K_{Ic} curve is plotted on each graph of fig. 7 (thick line) using the ΔT_{56J} values given in tab. 1 and the RT_{NDT} value of the unirradiated material ($RT_{NDT}^{unirr} = -27^\circ\text{C}$). It is shown that in the investigated range

$\Delta\sigma_Y / \text{MPa}$	$\Delta T_{56J} / ^\circ\text{C}$	$\Delta T_{K_{Ic},100} / ^\circ\text{C}$	$\Delta T_{K_{Ic},100} - \Delta T_{56J} / ^\circ\text{C}$
45	30	49	+19
88	56	73	+17
150	95	104	+9

Table 1
Comparison between ΔT_{56J} and predicted $\Delta T_{K_{Ic},100}$ shifts

for $\Delta\sigma_Y$, the model predictions are always less conservative than the ASME curve which remains a lower bound.

7 Discussion and conclusions

Simulation of the DBT curves for the unirradiated material.

The ductile to brittle transition characterized by the Charpy impact test and quasi-static fracture toughness test has been modeled in the case of a RPV steel using constitutive equations for viscoplasticity, ductile tearing and brittle failure. The whole Charpy and quasi-static fracture toughness transition curve of the base unirradiated material can be modeled provided the parameter σ_u of the Beremin model is considered to be an increasing function of temperature. This apparent effect of temperature on the cleavage mechanism is considered to be a combination of the effect of large plastic strain, temperature-induced inhomogeneity of local stress-strain fields and a possible change of the critical defects population. Moreover it should be reminded that the cleavage model considered in this study does not consider the microcracks nucleation step of the cleavage process (see e.g. [58]).

Simulation of the USE decrease due to irradiation.

The irradiation-induced USE decrease reported in many experimental studies cannot be reproduced considering only the increase of the hardening properties.

Following experimental results obtained on an A508 steel, the work hardening rate was considered to be unaffected by irradiation, at least in the fluence range considered here. Preliminary FE simulations of the Charpy test, not reported here, considering a decreasing hardening rate with irradiation (i.e. hypothesis irr. 2 on fig. 1a), show that the enhanced localization induced by a lower hardening rate is not able to compensate for the increase of the maximum load level induced by the increase of the yield strength. As the Charpy energy is given by the area under the load-deflection curve, the deflection being the same when the behavior is fully ductile, the amount of energy is more important. This results in a higher upper shelf level. It should be also noted that fully ductile failure is obtained on irradiated materials at higher testing temperatures. This will induce a decrease of the USE if irradiation hardening is not considered. However for high levels of irradiation where up to a 50% decrease of the USE is reported [46], this temperature effect will not be sufficient to explain such decrease. In that case a possible change of nucleation rate may also be involved in the observed decrease of the USE level. Assuming that only a mode I ductile fracture is prevalent, a larger nucleation rate will lead to an acceleration of the ductile damage, so that the ductile crack will propagate faster resulting in a lower energy for a given temperature. Numerically it has been shown in case of strain controlled nucleation, a decrease of the critical nucleation strain favors shear-type fracture (cup-cone or slant fracture) [59]. Consequently it may be inferred that the change of nucleation rate due to increasing irradiation would lead to larger shear lips on the fracture surface. This change of macroscopic fracture behavior may be linked to the decrease of the USE. Fractographic investigations of irradiated specimens have to be carried out to investigate this hypothesis.

Simulation of the embrittlement due to irradiation. Irradiation

hardens the material causing an increase of the stresses thus causing earlier brittle failure. Considering hypothesis irr. 1, this effect cannot account quantitatively for the whole experimental reference temperature shift $\Delta T_{56J}(\Phi)$. It is therefore necessary to consider that irradiation also affects σ_u and consequently the mean macroscopic cleavage stress. Irradiation effect is then equivalent to “a cooling of the material”, the $\sigma_u(T)$ curve being shifted toward higher temperatures. The micromechanical mechanism needs however to be identified. A first hypothesis which is actually under investigation is the interaction between the irradiation-induced plastic deformation and population of potential nuclei for cleavage.

Using the value of $\sigma_u(T + \Delta T_\Phi)$ determined from Charpy data, the shifts of fracture toughness index temperature for different level of hardening corresponding to different level of irradiation were found to be slightly higher than the corresponding shifts obtained from Charpy energy curves. These fracture toughness predictions were found to be in agreement with literature data. The difference decreases with increasing hardening. However it has been checked that the ASME K_{Ic} curve with $\Delta RT_{NDT} = \Delta T_{56J}$ remains a lower bound for the CT(1T) fracture toughness data.

Effect of the irradiation-induced hardening evolution on the predicted DBT shifts and USE. Assuming hypothesis irr. 2 would have led for a given deflection

to smaller stresses and consequently to lower cleavage failure probability. This implies that using σ_u determined for the unirradiated material would have led to a larger underestimation of the DBT shifts. Consequently the conclusion that the mean cleavage stress (i.e. σ_u) is affected by irradiation is valid whatever the chosen hypothesis. This also holds for the actual plastic behavior which is bounded by hypotheses irr. 1 and irr. 2. The computed ΔT_{Φ} shown on fig. 5 would have been larger. Concerning the USE prediction, using hypothesis irr. 2 would not have led to a decrease but to smaller increase. Consequently the conclusion that nucleation may be affected by irradiation is valid.

Acknowledgments

Financial support from Direction de la Sûreté des Installations nucléaires (DSIN) and Electricité de France (EdF) is acknowledged.

References

- [1] ASME, ASME Boiler and Pressure Vessel Code, Section XI, "Inservice inspection of nuclear power plant", American Society for Mechanical Engineers, 1995.
- [2] K. Onizawa, M. Suzuki, Comparison of transition temperature shifts between static fracture toughness and Charpy-v impact properties due to irradiation and post-irradiation annealing for Japanese A533B-1 steels, in: S. Rosinski, M. Grossbeck, T. Allen, A. Kumar (Eds.), Effects of radiation on materials: 20th Inter. Symp., ASTM STP 1405, 2001, pp. 79–96.
- [3] M. Kirk, M. Natishan, Shift in toughness transition temperature due to irradiation: ΔT_0 vs ΔT_{41J} , a comparison and rationalization of differences, in: IAEA meeting, specialists meeting on Master Curve testing and results, Prague, Czech Republic, 2001.
- [4] K. Mathur, A. Needleman, V. Tvergaard, 3D analysis of failure modes in the Charpy impact test, Modelling Simul. Mater. Sci. Eng. 2 (1994) 617–635.
- [5] M. Tahar, B. Tanguy, Y. Grandjean, R. Piques, CVN energy and fracture toughness of an A508 steel at low temperature, in: E. publishing (Ed.), Fracture from defects ECF12, Sheffield, 14–18 Septembre, 1998.
- [6] W. Schmitt, D. Sun, G. Bernauer, G. Nagel, New approaches to improve the RPV materials database, Nuc. Eng. Design 183 (1998) 1–8.
- [7] L. Folch, F. Burdekin, Application of coupled brittle–ductile model to study correlation between Charpy energy and fracture toughness values, Engng Fract Mech 63 (1999) 57–80.
- [8] A. Needleman, V. Tvergaard, Numerical modeling of the ductile–brittle transition, Int J Frac 101 (2000) 73–97.
- [9] A. Rossoll, C. Berdin, C. Prioul, Determination of the fracture toughness of a low alloy steel by the instrumented Charpy impact test, Int J Frac 115 (2002) 205–226.
- [10] A. Parrot, P. Forget, A. Dahl, Evaluation of fracture toughness from instrumented Charpy Impact tests for a reactor pressure vessel steel, in: Proceedings of PVP 2003, Fatigue, Fracture & Damage., Cleveland, Ohio, USA, 2003.
- [11] B. Tanguy, J. Besson, R. Piques, A. Pineau, Numerical Modeling of Charpy V–notch tests, in: D. François, A. Pineau (Eds.), From Charpy to present impact testing,ESIS Publication 30, 2002, pp. 461–468.
- [12] B. Tanguy, J. Besson, R. Piques, A. Pineau, Ductile to brittle transition of a A508 steel characterized by the Charpy impact test. Part—II: modeling of the Charpy transition curve, Engng Fract Mech 72/3 (2005) 413–434.
- [13] B. Tanguy, J. Besson, C. Bouchet, S. Bugat, Comparison of predicted transition temperature shifts between static fracture toughness and Charpy-V impact properties due to irradiation for an A508 pressure vessel steel, in: PVP ASME, San Diego, 2004.
- [14] F. M. Haggag, Effects of irradiation temperature on embrittlement of nuclear pressure vessel steels, in: A. S. Kumar, D. S. Gelles, R. K. Nanstad, E. A.

Little (Eds.), Effects of Radiation on Materials: 16th Inter. Symp., ASTM STP 1175, 1993, pp. 172–185.

- [15] M. Kirk, C. Santos, E. Eason, J. Wright, G. Odette, Updated embrittlement trend curve for reactor pressure vessels steels, in: Trans. of the 17th International Conference on Structural Mechanics in Reactor Technology (SMIRT 17)- Prague, Aug 17–22, Prague, Aug 17–22, 2003, pp. G01–5.
- [16] N. Hiranuma, N. Soneda, K. Dohi, S. Ishino, N. Dohi, H. Ohata, Mechanistic modeling of transition temperature shift of Japanese RPV materials, in: 30. MPA-Seminar – Stuttgart, 6. and 7 October 2004, 2004.
- [17] Y. A. Nikolaev, A. V. Nikolaeva, Y. I. Shtrombakh, Radiation embrittlement of low-alloy steels, *Int. J. Pres. Ves. and Piping* 79 (2002) 619–636.
- [18] M. Wagenhofer, H. P. Gunawardane, M. E. Natishan, Yield and toughness transition prediction for irradiated steels based on dislocation mechanics, in: S. T. Rosinski, M. L. Grossbeck, T. R. Allen, A. S. Kumar (Eds.), Effects of Radiation on Materials: 20th Inter. Symp., ASTM STP 1045, ASTM, 2001, pp. 97–108.
- [19] C. Brillaud, F. Hedin, In-service evaluation of French pressurized water reactor vessel steel, in: R. Stoller, A. Kumar, D. Gelles (Eds.), Effects of radiation on materials: 15th Inter. Symp., ASTM STP 1125, 1992, pp. 23–49.
- [20] C. Trouvain, Approches globale et locale de la rupture fragile d'un acier faiblement allié. Influence des ségrégations et de l'irradiation, Tech. rep., CEA, Saclay (1989).
- [21] EDF, Edf industry-nuclear generation division corporate laboratory, private communication (2003).
- [22] B. Margolin, A. Gulenko, V. Nikolaev, L. Ryadkov, A new engineering method for prediction of the fracture toughness temperature dependence for RPV steels, *Int. J. Pres. Ves. and Piping* 80 (2003) 817–829.
- [23] M. Al Mundheri, P. Soulat, A. Pineau, Irradiation embrittlement of a low alloy steel interpreted in terms of a local approach of cleavage fracture, *Fatigue Fract. Engng. Mater. Struct.* 12 (1) (1989) 19–30.
- [24] K. Farrell, R. Stoller, P. Jung, H. Ullmaier, Hardening of ferritic alloys at 288°C by electron irradiation, *J. Nuclear Materials* 279 (2000) 77–83.
- [25] T. Byun, K. Farrell, Irradiation hardening behavior of polycrystalline metals after low temperature irradiation, *J. Nuclear Materials* 326 (2004) 86–96.
- [26] G. Odette, T. Yamamoto, H. Rathbun, M. He, M. Hribernik, J. Rensman, Cleavage fracture and irradiation embrittlement of fusion reactor alloys: mechanisms, multiscale models, toughness measurements and implications to structural integrity assessment, *J. Nuclear Materials* 323 (2003) 313–340.
- [27] T. Byun, K. Farrell, Plastic instability in polycrystalline metals after low temperature irradiation, *Acta mater.* 52 (2004) 1597–1608.
- [28] D. Parks, Interpretation of irradiation effects on the fracture toughness of a pressure vessel steel in terms of crack tip stress analysis, *J. Engng Mater Technology* (1976) 30–36.
- [29] B. Tanguy, J. Besson, R. Piques, A. Pineau, Ductile to brittle transition of an A508 steel characterized by the Charpy impact test. Part—I: experimental

results, Engng Fract Mech 72/1 (2005) 49–72.

- [30] K. Farrell, T. Byun, N. Haschimoto, Deformation mode maps for tensile deformation of neutron-irradiated structural alloys, J. Nuclear Materials 335 (2004) 471–486.
- [31] C. Brillaud, Y. Grandjean, S. SAILLET, Vessel investigation program of CHOOZ A PWR reactor after shutdown, in: S. T. Rosinski, M. L. Grossbeck, T. R. Allen, A. S. Kumar (Eds.), Effects of Radiation on Materials: 20th Inter. Symp., ASTM STP 1045, ASTM, 2001, pp. 28–40.
- [32] M. Sokolov, R. Nanstad, Comparison of irradiation-induced shifts of K_{Jc} and Charpy impact toughness for reactor pressure vessel steels, Tech. rep., ORNL, NUREG/CR-6609 (2000).
- [33] ASTM-E1921, Standard test method for Determination of reference temperature, T_0 , for ferritic steels in the transition range, ASTM, Philadelphia, USA, 2001.
- [34] K. Wallin, T. Planman, M. Valo, R. Rintamaa, Applicability of miniature size bend specimens to determine the master curve reference temperature T_0 , Eng. Fract. Mech. 68 (2001) 1265–1296.
- [35] B. Tanguy, R. Piques, L. Laiarinandrasana, A. Pineau, Mechanical behaviour of A508 steel based on double nonlinear viscoplastic constitutive equation, in: D. Miannay, P. Costa, D. François, A. Pineau (Eds.), EUROMAT 2000, Advances in Mechanical Behaviour. Plasticity and Damage, Elsevier, 2000, pp. 499–504.
- [36] B. Tanguy, J. Besson, An extension of the Rousselier model to viscoplastic temperature dependant materials, Int J Frac 116 (2002) 81–101.
- [37] V. Tvergaard, Material failure by void growth to coalescence, Advances in Applied Mechanics 27 (1990) 83–151.
- [38] C. Chu, A. Needleman, Void nucleation effects in biaxially stretched sheets, J Engng Mater Technology 102 (1980) 249–256.
- [39] X. Zhang, J. Knott, The statistical modelling of brittle fracture in homogeneous and heterogeneous steel microstructures, Acta mater. 48 (2000) 2135–2146.
- [40] F. Beremin, A local criterion for cleavage fracture of a nuclear pressure vessel steel, Met. Trans. 14A (1983) 2277–2287.
- [41] W. Lefevre, G. Barbier, R. Masson, G. Rousselier, A modified beremin model to simulate the warm pre-stress effect, Nuc. Eng. Design 216 (2002) 27–42.
- [42] J. Besson, R. Foerch, Large Scale Object-Oriented Finite Element Code Design, Computer Methods in Applied Mechanics and Engineering 142 (1997) 165–187.
- [43] AFNOR, Essai de flexion par choc sur éprouvette Charpy. Partie 1 : méthode d’essai, Association française de normalisation, La Défense, France, 1990.
- [44] J. Böhmert, H.-W. Viehrig, A. Ulbricht, Correlation between irradiation-induced changes of microstructural parameters and mechanical properties of RPV steels, J. Nuclear Materials 334 (2004) 71–78.
- [45] M. Miller, P. Pareige, M. Burke, Understanding pressure vessel steels: an atom probe perspective, Mater. Charac. 44 (2000) 235–254.

- [46] B. Gurovich, E. Kuleshova, Y. Shtrombakh, O. Zabusov, E. Krasikov, Intergranular and intragranular phosphorus segregation in Russian pressure vessel steels due to neutron irradiation, *J. Nuclear Materials* 279 (2000) 259–272.
- [47] E. Kuleshova, B. Gurovich, Y. Shtrombakh, D. Erak, O. Lavrenchuk, Comparison of microstructural features of radiation embrittlement of VVER-440 and VVER-1000 reactor pressure vessel steels, *J. Nuclear Materials* 300 (2002) 127–140.
- [48] P. Auger, P. Pareige, S. Welzel, J.-C. Van Duysen, Synthesis of atom probe experiments on irradiation-induced solute segregation in French ferritic pressure vessel steels, *J. Nuclear Materials* 280 (2000) 331–344.
- [49] F. Beremin, Influence de la triaxialité des contraintes sur la rupture par déchirement ductile et la rupture fragile par clivage d'un acier doux, *Journal de mécanique appliquée* 4 (3) (1980) 327–342.
- [50] B. Margolin, V. Kostylev, Radiation embrittlement modelling for reactor pressure vessels steels: II. Ductile fracture toughness prediction, *Int. J. Pres. Ves. and Piping* 76 (1999) 731–740.
- [51] J. Faleskog, X. Gao, C. Shih, Cell model for nonlinear fracture analysis—I : Micromechanics calibration, *Int. J. of Fract.* 89 (1998) 355–373.
- [52] J. Faleskog, C. Shih, Micromechanics of coalescence—I. Synergistic effects of elasticity, plastic yielding and multi-size-scale voids, *J. Mech. Phys. Solids* 45 (1) (1996) 21–50.
- [53] G. Hahn, The influence of microstructure on brittle fracture toughness, *Met. Trans. A* 15A (1984) 947–959.
- [54] Hunter, C.W. and Williams, J.A., Fracture and tensile behavior of neutron-irradiated A533-B pressure vessel steel, *Nuc. Eng. Design* 17 (1971) 131–148.
- [55] B. Gurovich, E. Kuleshova, Y. Nikolaev, Y. Shtrombakh, Assessment of relative contributions from different mechanisms to radiation embrittlement of reactor pressure vessel steels, *J. Nuclear Materials* 246 (1997) 91–120.
- [56] C. Bouchet, B. Tanguy, J. Besson, S. Bugat, Prediction of the effects of neutron irradiation on the Charpy ductile to brittle transition curve of an A508 pressure vessel steel, *Comp. Mat. Science* 32 (2005) 294–300.
- [57] K. Farrell, T. Byun, Tensile properties of ferritic/martensitic steels irradiated in HFIR, and comparison with spallation irradiation data, *J. Nuclear Materials* 318 (2003) 274–282.
- [58] S. Bordet, A. Karstensen, D. Knowles, C. Wiesner, A new statistical local criterion for cleavage fracture in steel. part i: model presentation, *Engng Fract Mech* 72/3 (2005) 435–452.
- [59] M. Saje, J. Pan, A. Needleman, Void nucleation effects on shear localization in porous plastic solids, *Engng Fract Mech* 19 (1982) 162–182.